

Double-Hit Signature of Millicharged Particles in 3D segmented neutrino detector

Dmitry Gorbunov^{a,b}, Igor Krasnov^a, Yury Kudenko^{a,b,c}, Sergey Suvorov^{a,b,d}

^a*Institute for Nuclear Research of Russian Academy of Sciences, 117312 Moscow, Russia*

^b*Moscow Institute of Physics and Technology, 141700 Dolgoprudny, Russia*

^c*National Research Nuclear University (MEPhI), 115409 Moscow, Russia*

^d*LPNHE Paris, Sorbonne Universite, Universite Paris Diderot, CNRS/IN2P3, Paris 75252, France*

Abstract

We calculate the production of hypothetical millicharged particles (MCPs) of sub-GeV masses by the J-PARC proton beam in the framework of T2K and future T2HK neutrino oscillation experiments. Concentrating on the region of model parameter space, where an MCP can hit the near neutrino detector twice, we adopt this background-free signature to estimate the sensitivity of T2K and T2HK experiments to MCPs. We find that a previously inaccessible in direct searches region of charges $5 \times 10^{-4} - 10^{-2} e$ for MCP masses 0.1-0.5 GeV can be probed.

1. Electric charge quantization remains inexplicable within the Standard Model of particle physics and may point at some Grand Unified Theory. Therefore it is worth searching for new particles with a fractional electric charge, widely called millicharged particles (MCPs): their observation would imply either a misconception in model building [1] or presence of additional Abelian gauge symmetries in particle physics at high energy [2]. Even dark matter particles can carry a tiny electric charge, see e.g. [3], with specific consequences for cosmology, and so MCPs can e.g. leave imprints on the anisotropy pattern of the cosmic microwave background [4, 5].

All these make MCPs a physically well motivated example of feebly interacting massive particles (FIMPs), which may be light, naturally avoiding detection so far and requiring a new generation of high intensity frontier experiments [6, 7]. They may be specifically dedicated to searches for new physics projects like SHiP [8, 9], or may aim at another physics tasks but be capable of performing searches for FIMPs along with working on the main tasks. Among the latter are next generation experiments on neutrino oscillations, and accelerator neutrino experiments, like DUNE and T2HK, cover a wide range of MCP masses [10]. With huge statistics of protons hitting a target and highly sensitive near detectors primarily

Email addresses: gorby@ms2.inr.ac.ru (Dmitry Gorbunov), iv.krasnov@physics.msu.ru (Igor Krasnov), kudenko@inr.ru (Yury Kudenko), suvorov@inr.ru (Sergey Suvorov)

devised to control the neutrino fluxes these experiments perfectly meet the criteria of FIMP's hunters.

In this letter, we investigate T2K and T2HK prospects in searches for MCP using the upgraded T2K near detector. Generically neutrino detectors are not suited for the detection of FIMP, since its interaction inside the detector closely mimics that of neutrino. To circumvent this obstacle in a neutrino experiment, ArgoNeut, Ref. [11] suggested exploiting the signature of two subsequent hits inside the detector volume as an MCP candidate. It is feasible for not very tiny electric charge. Simple estimations show almost no background from neutrinos produced by the beams. For T2HK oscillation measurements with $N_{POT} = 2.7 \times 10^{22}$ protons on target to be collected for about 10 years of operation and the upgraded T2K near detector designed as described in Ref. [12], we find this signature very promising. In particular, in models with MCP masses $m_\chi \simeq 0.1 - 0.5 \text{ GeV}$ T2HK will be able to probe previously unattainable region of charges $\epsilon e \simeq 10^{-3} - 10^{-2} e$, where e is electron charge.

It should be mentioned that a dedicated experiment to search for MCPs at J-PARC with a sensitivity to ϵ of $\sim 10^{-4}$ was proposed in Ref [13]. The concept of the detector is based on the idea of a segmented detector comprised of long scintillator bars with a high photo-electron yield from ionization produced by a charged particle that travels along a bar.

2. A pair of MCPs can emerge through a virtual photon in meson decays. This is the main mechanism of the MCP production at JPARC, where a 30 GeV high intensity proton beam hits the carbon target [14] hence generating light mesons. Light vector flavourless mesons ρ, ω, ϕ , can exclusively decay into the MCP pair $\chi\bar{\chi}$ with branching ratios

$$\text{Br}(V \rightarrow \chi\bar{\chi}) = \epsilon^2 \cdot \text{Br}(X \rightarrow e^+e^-) \cdot \left(1 + 2\frac{m_\chi^2}{M_V^2}\right) \sqrt{1 - 4\frac{m_\chi^2}{M_V^2}}, \quad V \in \{\rho, \omega, \phi\} \quad (1)$$

obtained by modifying that into muon pair (due to the lepton universality the difference stems from the phase space only) [15, 16]. Pseudoscalar mesons π^0, η, η' produce a pair of MCPs only in three-body decays, which branching ratios are suppressed with respect to (1) by a phase space factor and additional coupling constants. Vector mesons can decay similarly. Two-body decays are kinematically preferable for a heavier MCP, however, the pseudoscalar mesons are easier to produce in proton collisions, and we account for the three-body processes as well. Their partial decay widths can be derived by generalizing those for electrons and muons in Refs. [17–20] (see also [21]),

$$\begin{aligned} \text{Br}(X \rightarrow Y\chi\bar{\chi}) &= \epsilon^2 \cdot \text{Br}(X \rightarrow Y\gamma) \cdot \frac{2\alpha}{3\pi} f_{X \rightarrow Y} \int_{4m_\chi^2}^{m_X^2} \frac{dm_{\chi\chi}^2}{m_{\chi\chi}^2} \left(1 + 2\frac{m_\chi^2}{m_{\chi\chi}^2}\right) \left(1 - 4\frac{m_\chi^2}{m_{\chi\chi}^2}\right)^{\frac{1}{2}} \\ &\quad \times \left(\left(1 + \frac{m_{\chi\chi}^2}{M_X^2 - M_Y^2}\right)^2 - 4\frac{m_{\chi\chi}^2 M_X^2}{(M_X^2 - M_Y^2)^2} \right)^{\frac{3}{2}} |F_{XY}(m_{\chi\chi}^2)|^2, \quad (2) \\ X \rightarrow Y &\in \{\pi \rightarrow \gamma, \eta \rightarrow \gamma, \eta' \rightarrow \gamma, \omega \rightarrow \pi^0, \phi \rightarrow \pi^0, \phi \rightarrow \eta\}, \\ f_{\pi \rightarrow \gamma} &= f_{\eta \rightarrow \gamma} = f_{\eta' \rightarrow \gamma} = 1, \quad f_{\omega \rightarrow \pi^0} = f_{\phi \rightarrow \pi^0} = f_{\phi \rightarrow \eta} = \frac{1}{2}, \end{aligned}$$

with $m_{\chi\chi}$ denoting the invariant mass of the MCP pair and form factors taken from Refs. [17–20, 22–24] as follows

$$|F_{\pi\gamma}(m_{\chi\chi}^2)|^2 = \left(1 + a_\pi \frac{m_{\chi\chi}^2}{M_\pi^2}\right)^2, \quad M_\pi = 0.135 \text{ GeV}, \quad a_\pi = 0.11 \quad (3)$$

$$|F_{\eta\gamma}(m_{\chi\chi}^2)|^2 = \left(1 - \frac{m_{\chi\chi}^2}{\Lambda_\eta^2}\right)^{-2}, \quad \Lambda_\eta = 0.72 \text{ GeV} \quad (4)$$

$$|F_{\eta'\gamma}(m_{\chi\chi}^2)|^2 = \frac{\Lambda_{\eta'}^2 (\Lambda_{\eta'}^2 + \gamma_{\eta'}^2)}{(\Lambda_{\eta'}^2 - m_{\chi\chi}^2)^2 + \Lambda_{\eta'}^2 \gamma_{\eta'}^2}, \quad \Lambda_{\eta'} = 0.79 \text{ GeV}, \quad \gamma_{\eta'} = 0.13 \text{ GeV} \quad (5)$$

$$|F_{\omega\pi^0}(m_{\chi\chi}^2)|^2 = \left(1 - \frac{m_{\chi\chi}^2}{\Lambda_\omega^2}\right)^{-2}, \quad \Lambda_\omega = 0.65 \text{ GeV} \quad (6)$$

$$|F_{\phi\eta}(m_{\chi\chi}^2)|^2 = \left(1 - \frac{m_{\chi\chi}^2}{\Lambda_{\phi\eta}^2}\right)^{-2}, \quad \Lambda_{\phi\eta}^{-2} = 1.93 \text{ GeV}^{-2} \quad (7)$$

$$|F_{\phi\pi^0}(m_{\chi\chi}^2)|^2 = \left(1 - \frac{m_{\chi\chi}^2}{\Lambda_{\phi\pi^0}^2}\right)^{-2}, \quad \Lambda_{\phi\pi^0} = 2.02 \text{ GeV}^{-2}. \quad (8)$$

The branching ratios entering Eqs. (1),(2) are given in [25] as

$$\begin{aligned} \text{Br}(\pi \rightarrow \gamma\gamma) &= 0.988, & \text{Br}(\eta \rightarrow \gamma\gamma) &= 0.394, & \text{Br}(\eta' \rightarrow \gamma\gamma) &= 0.0221 \\ \text{Br}(\rho \rightarrow e^+e^-) &= 4.72 \times 10^{-5}, & \text{Br}(\omega \rightarrow e^+e^-) &= 7.28 \times 10^{-5}, & \text{Br}(\phi \rightarrow e^+e^-) &= 2.95 \times 10^{-4} \\ \text{Br}(\omega \rightarrow \pi^0\gamma) &= 0.0828, & \text{Br}(\phi \rightarrow \pi^0\gamma) &= 1.27 \times 10^{-3}, & \text{Br}(\phi \rightarrow \eta\gamma) &= 0.0131 \end{aligned}$$

The corresponding partial decay ratios are presented in Fig. 1.

The light mesons are produced by protons scattering off the target and initiating hadronic showers. The meson spectra are estimated with the GEANT4 [26] package. The choice of the model of hadronic interactions affects this study, thus various physics lists were considered. The GEANT4 toolkit defines roughly two kinematic regions split with ≈ 10 GeV threshold where different models are applied. Above 10 GeV, the most widely used models in HEP are: Quark gluon string model (QGSP) and Fritiof (FTF). At the energy region below 10 GeV we considered BERTini (BERT) and binary cascade (BIC) models. The light meson production was estimated with all the above models and their results were compared. We found nearly no difference ($<1\%$) between the low-energy BERT and BIC models. While the predictions of QGSP and FTF were quite different. The results of the latter models are summarized in Table 1.

The QGSP_BERT physics list was considered more reliable as it provides better agreement with known T2K π^0 production and we use it in what follows. However, we found no experimental measurements of the production rates of other light mesons, thus the number of initial mesons is a possible source of uncertainties in the current study. The largest difference between the models was observed for ρ and ω yields. The kinematic distributions of the produced mesons are shown in Fig. (2).

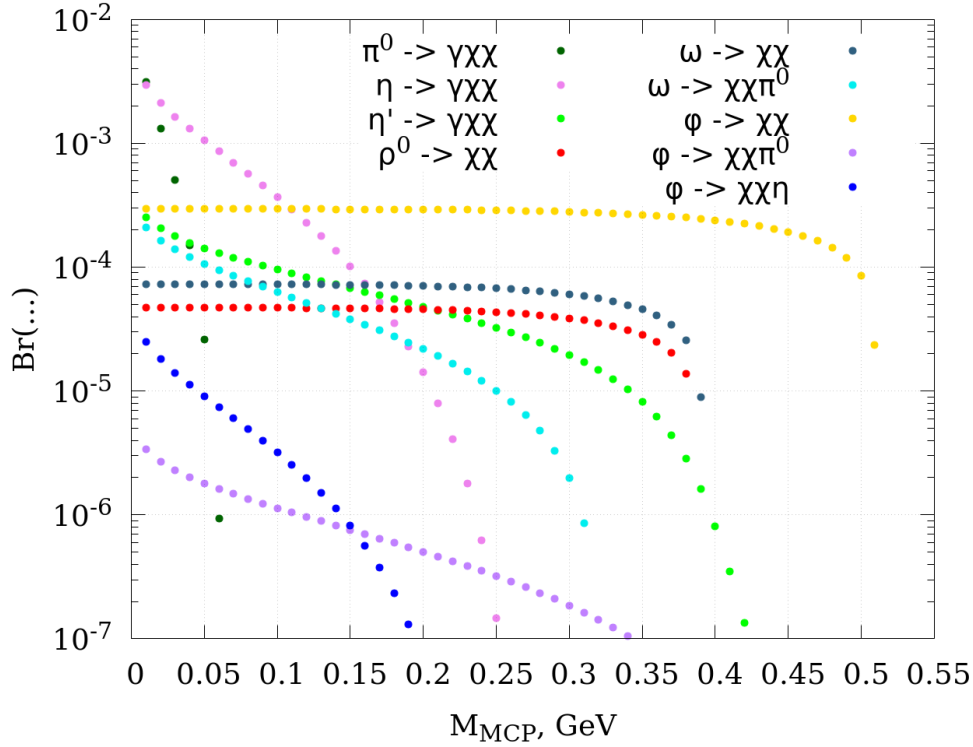


Figure 1: Meson branching ratios into MCP for $\epsilon^2 = 1$.

Meson	QGSP_BERT	FTF_BERT
π^0	3.12	4.17
η	0.40	0.31
η'	0.15	0.14
ρ	0.21	0.40
ω	0.12	0.27
ϕ	0.0051	0.0051

Table 1: The light meson production per initial 30 GeV proton collision with the T2K target for different GEANT4 physics lists.

We performed simulations for $N_{sim} = 2 \times 10^6$ protons on target (POT) which reveal the following (approximate) numbers of produced light mesons participating in the MCP phenomenology:

$$\begin{aligned}
 N_\pi &= 6.24 \times 10^6, & N_\eta &= 7.94 \times 10^5, & N_{\eta'} &= 2.96 \times 10^5, \\
 N_\rho &= 4.16 \times 10^5, & N_\omega &= 2.32 \times 10^5, & N_\phi &= 1.01 \times 10^4.
 \end{aligned}$$

Directions of outgoing MCPs are obtained 1) adopting isotropic distribution in the rest frame

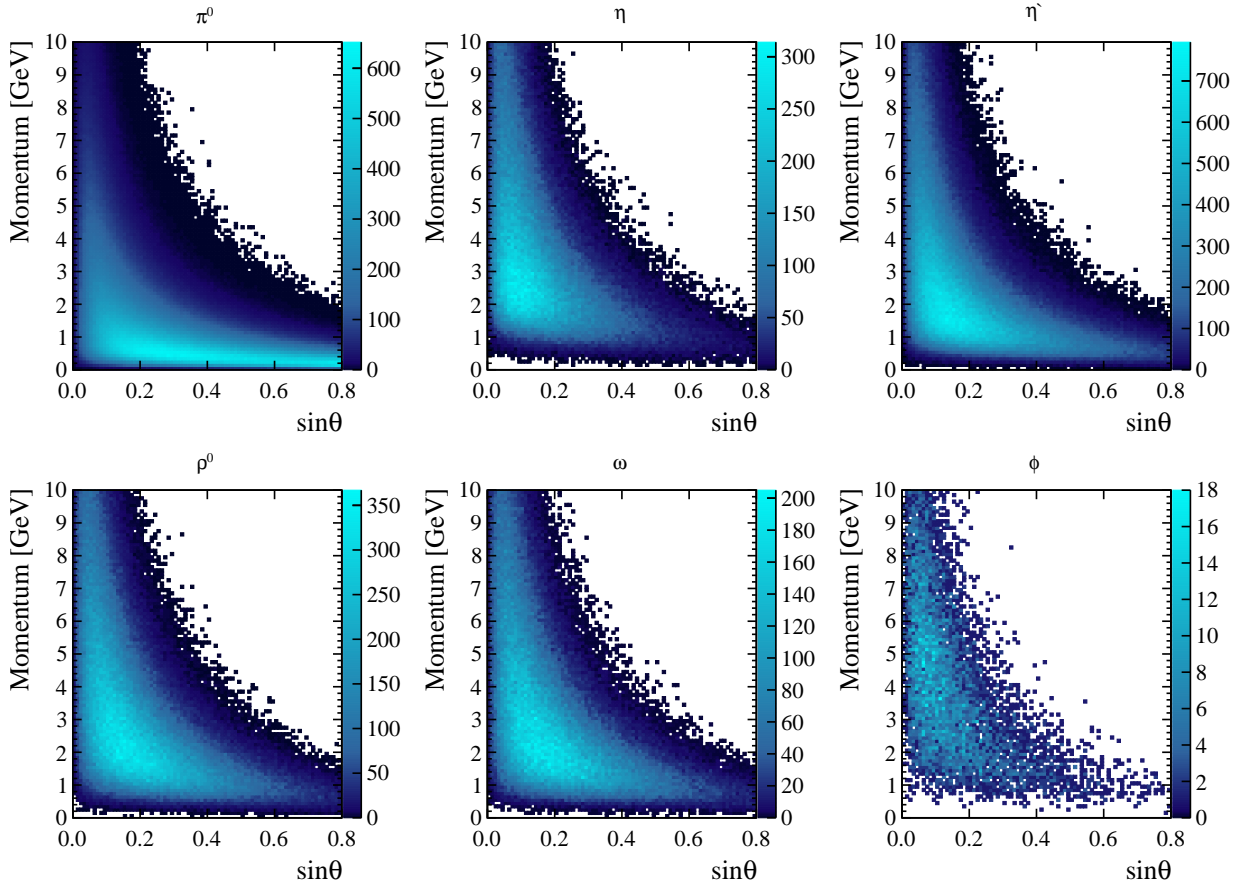


Figure 2: Light meson kinematic distributions over 3-momentum and angle with respect to the J-PARC proton beam.

of decaying mesons in case of two-body decays, and for the three-body decays we choose the invariant mass of MCPs (and thus the energy of the third particle) randomly in accordance with distribution (2) and assigning the third particle's momentum a random direction in the rest frame we restore the momenta of MCPs accordingly, and 2) performing the Lorentz transformation back to the laboratory system with a help of boost along the decaying meson 3-momentum. To be detected, the produced MCP must make the selected signature of two subsequent hits inside the detector volume, and so we require for the trajectory of observable MCP to pass through the T2K near detector, which is placed at a distance of $d = 280$ m from the target and at 2.5° off the proton beam axis.

3. For the MCP detection we consider the new neutrino detector SuperFGD [27] which will be installed inside the off-axis detector complex ND280. The main purpose of this detector is to reduce the systematic uncertainties in the prediction of a total number of signal neutrino events in the far T2K detector Super-Kamiokande, in presence of oscillations [12]. SuperFGD begins data taking within the T2K program, operating with Super-Kamiokande [28], and then will be used for measurement of CP asymmetry in neutrino oscillations with the Hyper-Kamiokande detector (T2HK program). The highly granular

scintillator detector SuperFGD of a mass of about 2 tons is comprised of $\sim 2 \times 10^6$ small scintillator cubes of 1 cm side, each read out with WLS fibers in the three orthogonal directions coupled to compact photosensors, Multi-Pixel Photon Counters (MPPCs), as shown in Fig. 3.

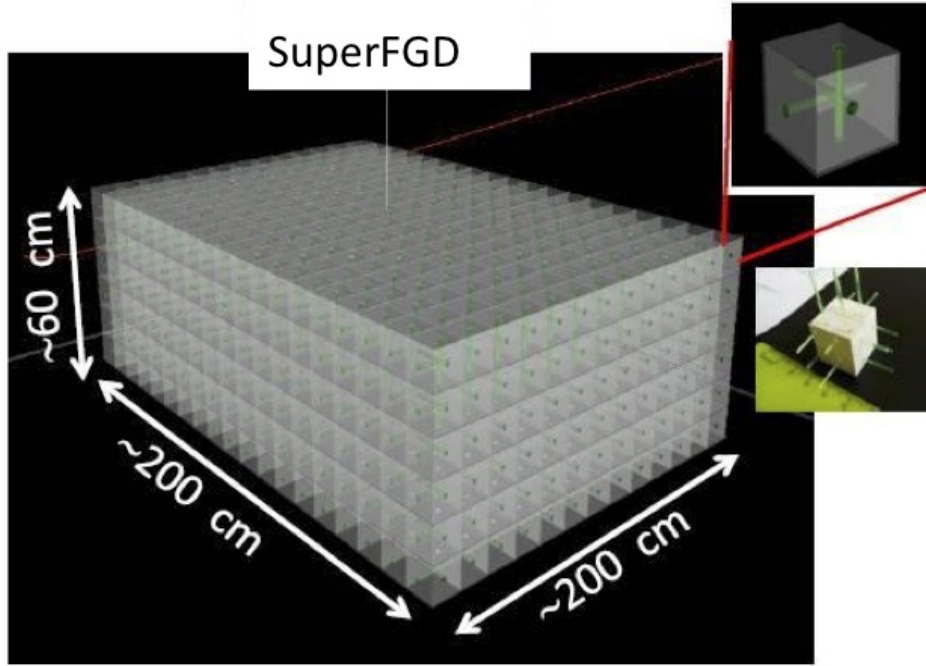


Figure 3: 3D view of the SuperFGD structure. Also shown are cubes of $1 \times 1 \times 1 \text{ cm}^3$ with 3 orthogonal wave-length shifting fibers inserted into holes.

SuperFGD will serve as an active neutrino target and a 4π detector of charged particles from neutrino interactions. The size of SuperFGD is about $0.56 \times 1.92 \times 1.84 \text{ m}^3$. A small angle 2.5° with respect to the neutrino beam doesn't cause a strong reduction of the MCP flux. The main acceptance limitation comes from the detector front surface area. The detector is placed so that its front side with respect to the beam has a size of $1.92 \times 0.56 \text{ m}^2$ and the 1.84 m side is oriented along the beam direction. We define a geometrical factor $\xi_{X,i}$ as the fraction of simulated MCP trajectories entering SuperFGD. These factors are calculated for each MCP production mode, the results are summarized for each parent meson in Fig. 4. The corresponding numbers and spectra of MCPs that reach the detector are presented in Fig. 5. One can check along the lines of Ref. [11] that for the reference value of $\epsilon = 10^{-3}$ the energy loss and trajectory deflections due to MCP multiple scattering in soil on the way of $\sim 200 \text{ m}$ to the detector are negligible.

Prototypes of SuperFGD were tested in a charged beam at CERN and showed a very good performance [29, 30]. Light yields per minimum ionizing particle (MIP) of 50-60 photoelectrons (p.e.) from individual cubes and from a single WLS fiber were obtained.

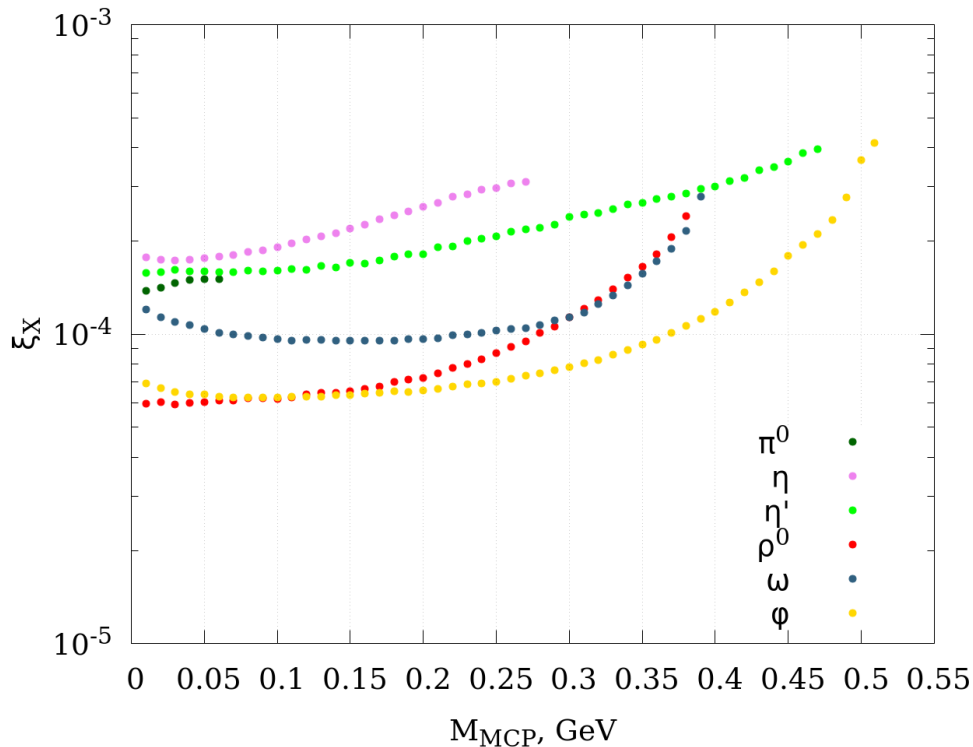


Figure 4: The geometrical factor $\xi_{X,i}$ for MCP as a function of its mass for each parent meson.

The sum of signals from 3 WLS fibers gives the total light yield of 150-180 p.e. per MIP for a single cube. Very good timing was also obtained in the beam tests. The time resolution of $\sigma \sim 1$ ns for an individual cube for the light yield corresponding to about 2 MeV energy deposited in this cube and measured by one WLS fiber. For 3 fiber readout the time resolution is expected to be about 0.6 ns in this case. For a larger than 2 MeV energy deposit in SuperFGD (more than 1 cube is fired) the time resolution should be better than 0.5 ns. This parameter is important for the suppression of the neutron background produced by the neutrino beam as discussed below.

SuperFGD will be equipped with Hamamatsu MPPCs S13360-1325 which have unique features: a very low dark rate of 60-70 kHz and 0.5 kHz at the threshold of 0.5 p.e. and 1.5 p.e., respectively, and a low cross-talk of about 1% [30]. The detection signature of MCPs in the SuperFGD detector is elastic scattering off atomic electrons, which results in knock-on δ -electrons above the detection threshold providing a detectable signal. Assuming that parameters of SuperFGD will be close to those obtained in the beam tests, one can expect that the energy of about 100 keV deposited by a recoil electron produces the light yield of 3.1-3.6 p.e. per a WLS fiber. Given this result, the efficiency to detect a 100 keV electron in one WLS fiber is estimated to be $\geq 82\%$ for the threshold of 1.5 p.e. Since about 99% of recoil electrons have energies from 0.1 MeV to 10 MeV, the total efficiency to detect recoil

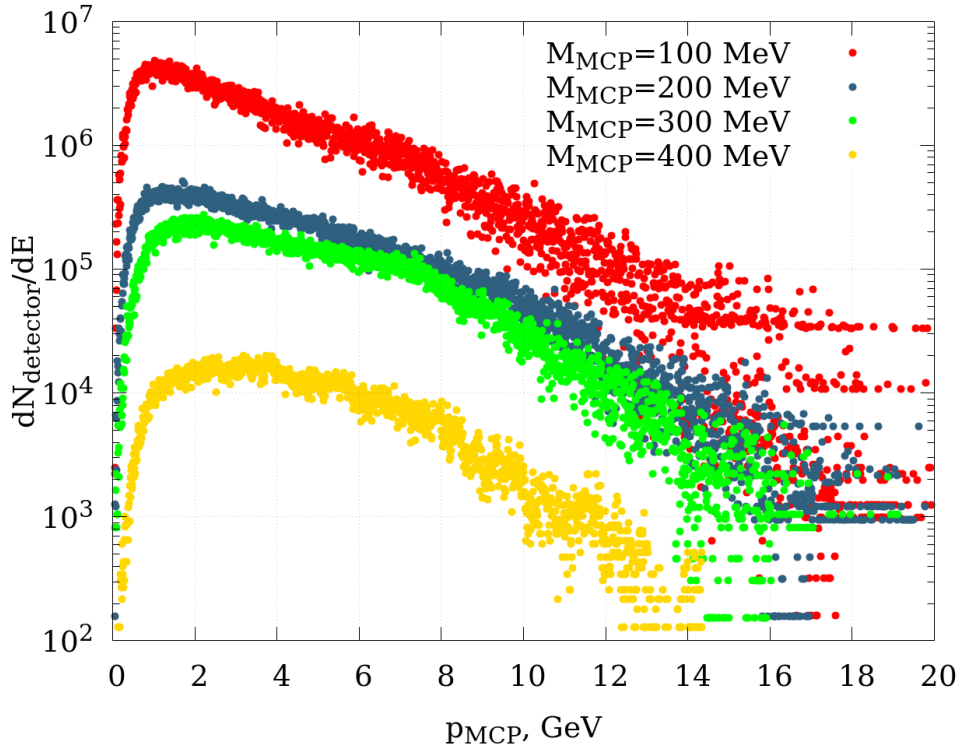


Figure 5: The spectra of MCPs that reach the SuperFGD for a set of masses and $\epsilon = 10^{-3}$. Integrating the spectrum over E reveals the total number of MCPs that pass through the detector for $N_{POT} = 3.2 \times 10^{22}$: 2.01×10^9 for $M_{MCP} = 100$ MeV, 2.63×10^8 for $M_{MCP} = 200$ MeV, 1.58×10^8 for $M_{MCP} = 300$ MeV, 1.15×10^7 for $M_{MCP} = 400$ MeV.

electrons by one WLS fiber is estimated to be about 98%. As a result, one can expect to reach the MCP detection efficiency in an individual cube of about 96% for a coincidence of signals from two WLS fibers for the energy threshold of $E_r^{min} = 100$ keV. The idea to detect MCPs lays in using two separated hits from an MCP aligned with the upstream meson production target. This method, proposed in Ref. [11] and used for a search of MCPs in the ArgoNeuT experiment [31], allows us to achieve a good background rejection, as seen below.

4. It is important to investigate a two-hit background in SuperFGD from several sources. Signals caused by random electronics noise due to the MPPC dark rate can mimic the MCP signal. Assuming the mentioned above MPPC dark rate of 0.5 kHz for the threshold of 1.5 p.e., the time window of 30 ns for each readout channel, and the two-fiber readout (both fibers are perpendicular to the beam direction) one can obtain the counting rate of about $1.5 \times 10^{-2} \text{ s}^{-1}$ due to coincidence of noise signals from two MPPCs. The total dark rate from all 2×10^6 SuperFGD cubes will be about $3 \times 10^4 \text{ s}^{-1}$. Since the accidental hit events will be uniformly distributed in SuperFGD volume they will only rarely align with the meson production target. To estimate the number of two electronic noise hits (two distant cubes in a line with the production target provides signals above the threshold of 1.5 p.e.) we

assume that the second hit occurs inside a 5×5 cluster in a column of about 100 cubes that forms a straight line with the first cluster and the target. The rate of such coincidence is estimated to be $\leq 4 \times 10^{-12} \text{ s}^{-1}$. Taking into account the beam structure with the spill width of $5 \mu\text{s}$ and the repetition period of 2.48 s for T2K (1.16 s for T2HK) [28], accidentals in a cube due to the dark rate of MPPCs are expected to be suppressed by a factor of 2×10^{-6} for T2K and $< 5 \times 10^{-6}$ for T2HK. Assuming 2.7×10^{22} POT for Hyper-Kamiokande that corresponds to about 10^8 s of data taking, the expected total number of background events due to the random electronics noise is $\leq 10^{-4}$.

Another source of accidental background can be the coincidence between the signal from a cube where MPPCs dark rate mimics the MCP signal (the first hit) and the real MCP signal from its interaction in SuperFGD (the second hit). Assuming the interaction length of MCP ($\epsilon = 10^{-3}$) is about $1.3 \times 10^6 \text{ cm}^2$, for a cluster of 5×5 cubes which is on a straight line with the first cluster and the target, one can obtain the number of such coincidences is about 2.5×10^{-2} for running time of 10^8 s.

The vast majority of neutrino induced events, for example, double-hit events from muon (electron) and neutron in the case of ν_μ charge current quasi elastic scattering (CCQE) will provide signals with a large number of cubes fired. By implementing the requirement that the track length should be ≤ 5 cubes that corresponds to the electron energy deposit of $\leq 10 \text{ MeV}$ these neutrino induced backgrounds can be significantly reduced.

The neutral current reactions in SuperFGD

$$\nu + {}^{12}\text{C} \rightarrow \nu' + {}^{11}\text{C}^* + n \quad (9)$$

and

$$\nu + {}^{12}\text{C} \rightarrow \nu' + {}^{11}\text{C} + n \quad (10)$$

are the most serious sources of background. There are no measurements of these cross sections on ${}^{12}\text{C}$ at the T2K neutrino energies, but for the background estimation, we can use the value of the neutral-current elastic-like cross section on oxygen $\sim 10^{-38} \text{ cm}^2$ measured by T2K [32] via detecting nuclear de-excitation γ -rays at Super-Kamiokande.

The excited ${}^{11}\text{C}^*$ emits γ -rays promptly and relaxes to the ground state. Assuming that the detection efficiency of γ -rays produced from the de-excitation of ${}^{12}\text{C}^*$ is 100%, one can find that about 3×10^5 such events will be detected in SuperFGD for 2.7×10^{22} POT. The neutron from the reaction (9) can mimic the MCP signal if its hit is in coincidence with the neutrino interaction vertex time, both neutrino and neutron vertexes align with the target, and neutron deposits the energy of $\leq 15 \text{ MeV}$ in its interaction because less than 1% of knock-on δ -electrons from the MCP interaction have the energy exceeding 15 MeV. Taking into account the time-of-flight between the first signal (de-excitation of ${}^{11}\text{C}^*$) and the second one from the scattered neutron, these background events will be suppressed using excellent time resolution of $\sigma \sim 0.2 - 0.3 \text{ ns}$. It can be obtained for events in which several cubes are fired that corresponds to energies of a few MeV. Neutrons with the kinetic energy below 300 MeV (about 90% of all events) are estimated to be rejected by a factor of 10^4 with the time-of-flight method. Neutrons in the energy range 300-600 MeV can be suppressed by three orders of magnitude. A small amount of neutrons with energies exceeding 600 MeV

($< 10^{-2}$) will be rejected by about 20 times. The requirement for protons from (n, p) scattering to have the kinetic energy of ≤ 15 MeV gives an additional suppression factor of about 10. The cross section of the reaction (10) with ^{11}C in the ground state is several times smaller than the cross section of (9). To mimic the MCP event, the neutron from this reaction should interact two times in the SuperFGD and pass through all selection criteria. Using the approach applied for the reduction of the background from the reaction (9), the background from the reaction (10) is expected to be suppressed to a much lower level.

Neutrons produced by the beam neutrinos in the sand around the ND280 pit and in the ND280 magnet interact many times and are slowed down during the propagation. A large fraction of reached SuperFGD neutrons are delayed with respect to the neutrino interaction time and produce signals between the beam bunches and microbunches (8 microbunches each of about 50 ns separated by 700 ns fill a beam bunch of 5 μs). Events in which neutrons coincide with the beam spill and interact 2 times in SuperFGD will be suppressed by the time-of-flight method and the required alignment of two hits with the target.

In total, we can expect less than 0.1 event contribution to the MCP background from the neutron current interactions in SuperFGD. These estimations of background rates are used to calculate the expected sensitivity of SuperFGD to MCPs. Eventually, the background will be determined from the data accumulated with the neutrino beam.

5. Upon entering the detector, an MCP can scatter off the material electrons. The recoil electrons can be observed, if the recoil energy is above a certain threshold E_r^{min} , and so the interesting cross section $\sigma(E_r^{min})$ depends on the energy carrying away by the electron. In the limit of a relativistic MCP the mean free path of MCP inside material with electron density Zn_{det} reads [10]

$$\lambda = \frac{1}{Zn_{det}\sigma(E_r^{min})} = \epsilon^{-2} \frac{m_e E_r^{min}}{2\pi\alpha^2 Zn_{det}}. \quad (11)$$

For SuperFGD (made up of carbon-based scintillator) we have $Z = 7$, and the matter density is $\rho_{ND} = 1.0 \frac{\text{g}}{\text{cm}^3}$ with molar mass $m_a(CH) = 13.0 \frac{\text{g}}{\text{mol}}$ [30], and hence $n_{det} = \frac{\rho_{ND}}{m_a(CH)} = 4.64 \times 10^{22} \text{cm}^{-3}$. Consequently, for the MCP mean free path one obtains

$$\lambda \approx 1.2 \times 10^4 \times \left(\frac{10^{-3}}{\epsilon}\right)^2 \times \left(\frac{E_r^{min}}{100 \text{keV}}\right) \text{m}.$$

normalized to the expected SuperFGD threshold of the electron recoil energy $E_r^{min} = 100 \text{keV}$.

In this study, we utilize a double-hit signature: the MCP has to scatter twice inside the detector, each time transferring to electron the energy above the threshold E_r^{min} . The possibility of 2 consecutive hits, each observed with efficiency ξ , is [10]:

$$P_{2h} = \frac{1}{2} \left(\xi \frac{L}{\lambda}\right)^2 = \frac{1}{2} \left(\frac{0.96 \times \left(\frac{\xi}{0.96}\right) 1.84 \text{m}}{\left(\frac{10^{-3}}{\epsilon}\right)^2 \left(\frac{E_r^{min}}{100 \text{keV}}\right) 12 \text{km}}\right)^2 \approx 1.1 \times 10^{-8} \times \left(\frac{\epsilon}{10^{-3}}\right)^4. \quad (12)$$

The detection efficiency ξ of each MCP hit with the electron energy ≥ 100 keV is estimated to be about 96%. Remarkably, the probability to produce the chosen signature does not depend on the MCP production channel.

6. At this stage we can sum up contributions of various production modes to the number of signal events N_S . Our estimate of N_S is based on the described above GEANT4 simulation of the production of the meson of type X , its branching ratios in a particular decay mode $\text{Br}_i(X \rightarrow \dots)$, and calculation of the corresponding geometrical factor $\xi_{X,i}$, as follows

$$N_S = N_{POT} \times \sum_X \frac{N_X}{N_{sim}} \times \sum_i \text{Br}_i(X \rightarrow \dots) \times \xi_{X,i} \times P_{2h}.$$

In Fig. 6 we plot for each parent meson the number of expected events for MCP reference

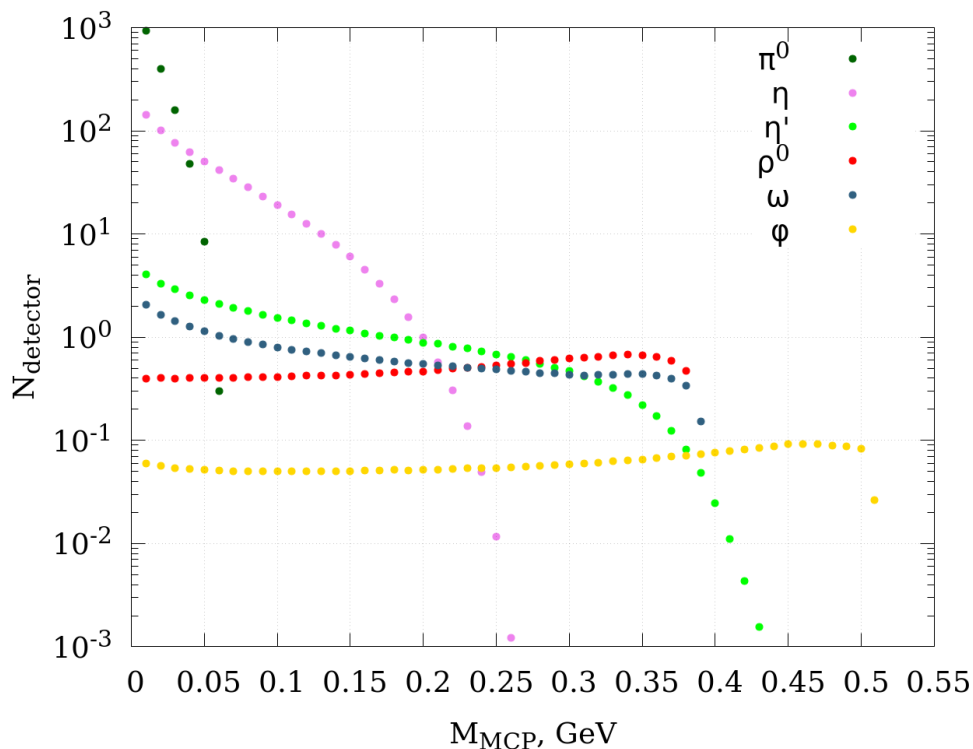


Figure 6: The simulated number of the double-hit MCP events in SuperFGD for various parent mesons and $\epsilon = 10^{-3}$.

model with $\epsilon = 10^{-3}$. Since the signature we adopt depends on neither energy nor mass of the MCP, we can estimate the total number of expected signal events in SuperFGD for each MCP mass simply summing over all the production channels. Requiring this number to be smaller than 3 we estimate the T2HK sensitivity (at 95% CL) to the MCP charge: the region above the black dots in Fig. 7 will be excluded after 10 years of data taking (in case

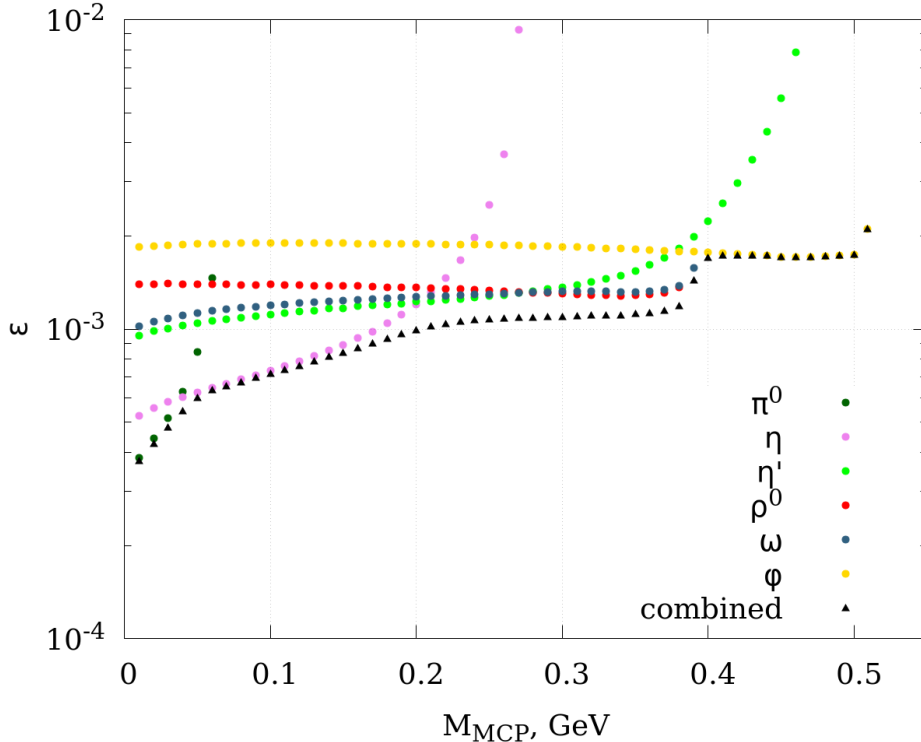


Figure 7: The expected exclusion regions (above the dots) of ϵ in case of 3 signal events and no background.

of no signal). We draw the exclusion curves for each parent meson to illustrate for which MCP mass they give a dominating contribution.

7. To conclude, in this paper we propose to use the double-hit signature of hypothetical millicharged particles at presently under construction SuperFGD Near Detector of T2K-T2HK long-base line neutrino experiment. We evaluate the production of MCP particles and trace their trajectory passing through the detector. We argue that the signature is background free for the expected T2HK statistics of protons on target. Since SuperFGD will operate for a few years within the T2K program and then switch to the T2HK program we calculate the expected number of events for both stages of operation, assuming 0.5×10^{22} POT and 2.7×10^{22} POT respectively. Assuming no signal events to be observed and exploiting the Poisson statistics we present in Fig. 8 the expected sensitivities (95% CL exclusion regions) for T2K and for the sum of both T2K and T2HK experiments. There are also limits placed by dedicated searches of MiiliQ@SLAC [33] and ArgoNeuT [31] and specific analyses of other accelerator data, including recent LHC results [34]. Also, results of the Super-K experiment were used in Ref. [36] to constrain the model parameter space, considering possible MCP production by cosmic rays. While it is similar to the ArgoNeuT results, there are significant uncertainties associated with the description of the propagation and interaction of the particles in the atmosphere and a more detailed analysis of the sig-

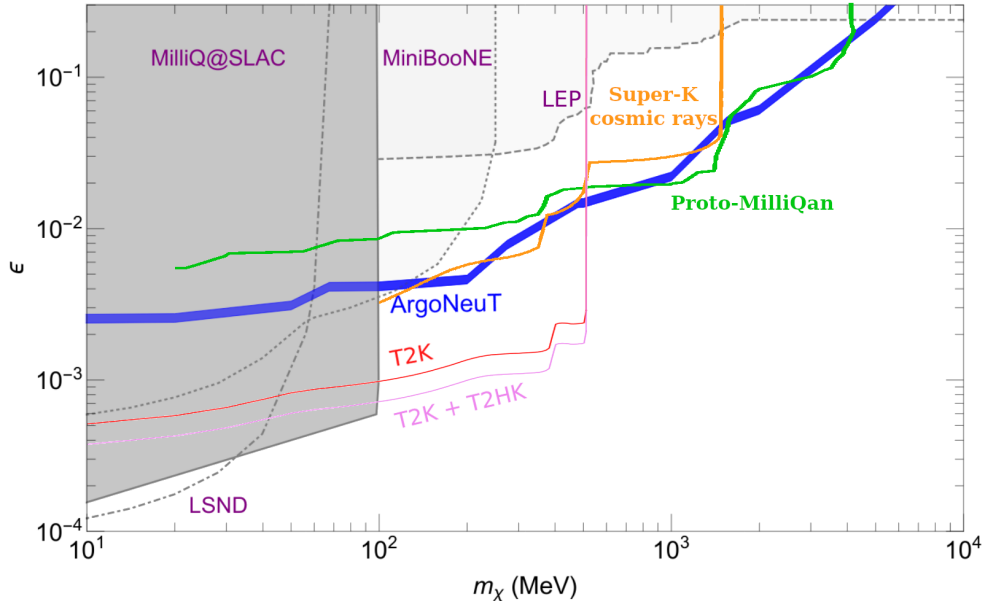


Figure 8: The expected sensitivity of T2K and T2HK to models with millicharged particles. The regions indicated by MilliQ@SLAC [33] and ArgoNeuT [31], recent LHC results (Proto-MilliQan) [34] are excluded by the corresponding collaborations. There are also regions disfavored after reanalysis of published results by MiniBooNE, LSND, [10] and LEP, see e.g. [35], and analysis of the Super-K results with cosmic rays producing the MCPs [36].

nal signature and associated background conditions would be appropriate. The suggested searches at T2K and T2HK will investigate untouched by those searches region of masses 100-500 MeV and charges as low as $\sim 5 \times 10^{-4}$ of the electron charge. Recently it was argued [37] that a noticeable part of this region is disfavored from the results of the BEBC experiment operated in the 1980s at CERN.

The sensitivity is obtained assuming the negligible background, for chosen cuts on the recoil electron energy and the expected detection efficiency. All that should be checked after the commissioning stage of SuperFGD, which may allow one to optimize our set of cuts and efficiencies and further refine the obtained sensitivity. Special attention should be paid to the background from non-relativistic neutrons since the signal recoil events are in a rather low, sub-MeV energy range.

There are also some uncertainties on the theoretical side of calculations that are associated with the observed dependence of GEANT4 simulations of the meson production on the chosen QCD model.

However, since the number of signal events scales as the sixth power of the MCP charge, the overall uncertainty of the presented in Fig. 8 sensitivity is small, and our predictions are robust. At the same time, this strong dependence on the MCP charge makes any further improvement in the presented techniques rather fruitless. To investigate models with a light particle of smaller electric charge one must rely on other signatures with the number of

signal events involving lower powers of MCP charges, the *potentially* most promising is just missing energy, so the number of events is proportional to the squared charge only, like e.g. in ongoing NA64 [38].

We thank C.K.Jung, M.Khabibullin, T.Matsubara for valuable discussions and M. Kirsanov, N. Starkov for clarification on GEANT4 packages. This work is supported in the framework of the State project “Science” by the Ministry of Science and Higher Education of the Russian Federation under the contract 075-15-2020-778.

References

- [1] L. B. Okun, M. B. Voloshin, and V. I. Zakharov, “ELECTRICAL NEUTRALITY OF ATOMS AND GRAND UNIFICATION MODELS,” *Phys. Lett.* **138B** (1984) 115–120.
- [2] B. Holdom, “Two U(1)’s and Epsilon Charge Shifts,” *Phys. Lett.* **166B** (1986) 196–198.
- [3] J. M. Cline, Z. Liu, and W. Xue, “Millicharged Atomic Dark Matter,” *Phys. Rev.* **D85** (2012) 101302, [arXiv:1201.4858 \[hep-ph\]](#).
- [4] S. L. Dubovsky and D. S. Gorbunov, “Small second acoustic peak from interacting cold dark matter?,” *Phys. Rev.* **D64** (2001) 123503, [arXiv:astro-ph/0103122 \[astro-ph\]](#).
- [5] S. L. Dubovsky, D. S. Gorbunov, and G. I. Rubtsov, “Narrowing the window for millicharged particles by CMB anisotropy,” *JETP Lett.* **79** (2004) 1–5, [arXiv:hep-ph/0311189 \[hep-ph\]](#). [Pisma Zh. Eksp. Teor. Fiz.79,3(2004)].
- [6] R. Essig *et al.*, “Working Group Report: New Light Weakly Coupled Particles,” in *Proceedings, 2013 Community Summer Study on the Future of U.S. Particle Physics: Snowmass on the Mississippi (CSS2013): Minneapolis, MN, USA, July 29-August 6, 2013*. 2013. [arXiv:1311.0029 \[hep-ph\]](#). <http://www.slac.stanford.edu/econf/C1307292/docs/IntensityFrontier/NewLight-17.pdf>.
- [7] P. Agrawal *et al.*, “Feebly-Interacting Particles:FIPs 2020 Workshop Report,” [arXiv:2102.12143 \[hep-ph\]](#).
- [8] S. Alekhin *et al.*, “A facility to Search for Hidden Particles at the CERN SPS: the SHiP physics case,” *Rept. Prog. Phys.* **79** no. 12, (2016) 124201, [arXiv:1504.04855 \[hep-ph\]](#).
- [9] SHiP Collaboration, M. Anelli *et al.*, “A facility to Search for Hidden Particles (SHiP) at the CERN SPS,” [arXiv:1504.04956 \[physics.ins-det\]](#).
- [10] G. Magill, R. Plestid, M. Pospelov, and Y.-D. Tsai, “Millicharged particles in neutrino experiments,” *Phys. Rev. Lett.* **122** no. 7, (2019) 071801, [arXiv:1806.03310 \[hep-ph\]](#).
- [11] R. Harnik, Z. Liu, and O. Palamara, “Millicharged Particles in Liquid Argon Neutrino Experiments,” *JHEP* **07** (2019) 170, [arXiv:1902.03246 \[hep-ph\]](#).
- [12] T2K Collaboration, K. Abe *et al.*, “T2K ND280 Upgrade - Technical Design Report,” [arXiv:1901.03750 \[physics.ins-det\]](#).
- [13] J. H. Kim, I. S. Hwang, and J. H. Yoo, “Search for sub-millicharged particles at J-PARC,” [arXiv:2102.11493 \[hep-ex\]](#).
- [14] T2K Collaboration, K. Abe *et al.*, “The T2K Experiment,” *Nucl. Instrum. Meth.* **A659** (2011) 106–135, [arXiv:1106.1238 \[physics.ins-det\]](#).
- [15] Y. M. Antipov *et al.*, “On Measurement of $\rho^0 \rightarrow \mu^+\mu^-$ Decay Branching Ratio in Coherent Dissociation Processes $\pi^- \rightarrow \mu^+\mu^-\pi^-$ and $\pi^- \rightarrow \pi^+\pi^-\pi^-$,” *Z. Phys. C* **42** (1989) 185.
- [16] KLOE Collaboration, F. Ambrosino *et al.*, “Measurement of the DAFNE luminosity with the KLOE detector using large angle Bhabha scattering,” *Eur. Phys. J. C* **47** (2006) 589–596, [arXiv:hep-ex/0604048](#).
- [17] BESIII Collaboration, M. Ablikim *et al.*, “Observation of the Dalitz Decay $\eta' \rightarrow \gamma e^+ e^-$,” *Phys. Rev.* **D92** no. 1, (2015) 012001, [arXiv:1504.06016 \[hep-ex\]](#).
- [18] NA60 Collaboration, R. Arnaldi *et al.*, “Precision study of the $\eta \rightarrow \mu^+\mu^-\gamma$ and $\omega \rightarrow \mu^+\mu^-\pi^0$

- electromagnetic transition form-factors and of the $\rho \rightarrow \mu^+\mu^-$ line shape in NA60,” *Phys. Lett.* **B757** (2016) 437–444, [arXiv:1608.07898 \[hep-ex\]](#).
- [19] **KLOE-2** Collaboration, D. Babusci *et al.*, “Study of the Dalitz decay $\phi \rightarrow \eta e^+e^-$ with the KLOE detector,” *Phys. Lett.* **B742** (2015) 1–6, [arXiv:1409.4582 \[hep-ex\]](#).
- [20] **KLOE-2** Collaboration, A. Anastasi *et al.*, “Measurement of the $\phi \rightarrow \pi^0 e^+e^-$ transition form factor with the KLOE detector,” *Phys. Lett.* **B757** (2016) 362–367, [arXiv:1601.06565 \[hep-ex\]](#).
- [21] K. J. Kelly and Y.-D. Tsai, “Proton fixed-target scintillation experiment to search for millicharged dark matter,” *Phys. Rev. D* **100** no. 1, (2019) 015043, [arXiv:1812.03998 \[hep-ph\]](#).
- [22] R. I. Dzhelyadin *et al.*, “Investigation of η Meson Electromagnetic Structure in $\eta \rightarrow \mu^+\mu^-\gamma$ Decay,” *Phys. Lett.* **94B** (1980) 548. [*Sov. J. Nucl. Phys.*32,516(1980); *Yad. Fiz.*32,998(1980)].
- [23] A. Beddall, “Measurement of the Dalitz-decay branching ratio of the π^0 ,” *Eur. Phys. J. C* **54** (2008) 365–370.
- [24] M. A. Schardt, J. S. Frank, C. M. Hoffman, R. E. Mischke, D. C. Moir, and P. A. Thompson, “A New Measurement of the Dalitz Decay Branching Ratio of the π^0 ,” *Phys. Rev. D* **23** (1981) 639.
- [25] **Particle Data Group** Collaboration, P. A. Zyla *et al.*, “Review of Particle Physics,” *PTEP* **2020** no. 8, (2020) 083C01.
- [26] **GEANT4** Collaboration, S. Agostinelli *et al.*, “GEANT4—a simulation toolkit,” *Nucl. Instrum. Meth.* **A506** (2003) 250–303.
- [27] A. Blondel *et al.*, “A fully active fine grained detector with three readout views,” *JINST* **13** no. 02, (2018) P02006, [arXiv:1707.01785 \[physics.ins-det\]](#).
- [28] **Hyper-Kamiokande** Collaboration, K. Abe *et al.*, “Hyper-Kamiokande Design Report,” [arXiv:1805.04163 \[physics.ins-det\]](#).
- [29] O. Mineev *et al.*, “Parameters of a fine-grained scintillator detector prototype with 3D WLS fiber readout for a T2K ND280 neutrino active target,” *Nucl. Instrum. Meth.* **A936** (2019) 136–138.
- [30] A. Blondel *et al.*, “The SuperFGD Prototype Charged Particle Beam Tests,” *JINST* **15** no. 12, (2020) P12003, [arXiv:2008.08861 \[physics.ins-det\]](#).
- [31] **ArgoNeuT** Collaboration, R. Acciarri *et al.*, “Improved Limits on Millicharged Particles Using the ArgoNeuT Experiment at Fermilab,” *Phys. Rev. Lett.* **124** no. 13, (2020) 131801, [arXiv:1911.07996 \[hep-ex\]](#).
- [32] **T2K** Collaboration, K. Abe *et al.*, “Measurement of neutrino and antineutrino neutral-current quasielasticlike interactions on oxygen by detecting nuclear deexcitation γ rays,” *Phys. Rev.* **D100** no. 11, (2019) 112009, [arXiv:1910.09439 \[hep-ex\]](#).
- [33] A. A. Prinz *et al.*, “Search for millicharged particles at SLAC,” *Phys. Rev. Lett.* **81** (1998) 1175–1178, [arXiv:hep-ex/9804008 \[hep-ex\]](#).
- [34] A. Ball *et al.*, “Search for millicharged particles in proton-proton collisions at $\sqrt{s} = 13$ TeV,” *Phys. Rev. D* **102** no. 3, (2020) 032002, [arXiv:2005.06518 \[hep-ex\]](#).
- [35] S. Davidson, S. Hannestad, and G. Raffelt, “Updated bounds on millicharged particles,” *JHEP* **05** (2000) 003, [arXiv:hep-ph/0001179 \[hep-ph\]](#).
- [36] R. Plestid, V. Takhistov, Y.-D. Tsai, T. Bringmann, A. Kusenko, and M. Pospelov, “New Constraints on Millicharged Particles from Cosmic-ray Production,” *Phys. Rev. D* **102** (2020) 115032, [arXiv:2002.11732 \[hep-ph\]](#).
- [37] G. Marocco and S. Sarkar, “Blast from the past: Constraints on the dark sector from the BEBC WA66 beam dump experiment,” *SciPost Phys.* **10** (2021) 043, [arXiv:2011.08153 \[hep-ph\]](#).
- [38] S. N. Gninenko, D. V. Kirpichnikov, and N. V. Krasnikov, “Probing millicharged particles with NA64 experiment at CERN,” *Phys. Rev.* **D100** no. 3, (2019) 035003, [arXiv:1810.06856 \[hep-ph\]](#).